Thermal lens measurement of Oxotrichlorobis(triphenylphosphine)rhenium(V) by CW laser beam

M. D. ZIDAN[1,*], M. M. AL-KTAIFANI[2], A. ALLAHHAM[1]
[1]*Department of Physics, Atomic Energy Commission, P. O. Box 6091, Damascus, Syria*
[2]*Department of Radioisotopes, Atomic Energy Commission, P. O. Box 6091, Damascus, Syria*

The thermal lens properties of Oxotrichlorobis(triphenylphosphine) rhenium(V) solution were explored using the dual-beam CW laser (pump-probe beams) z-scan. Then, a numerical model utilizes to performed theoretical calculation in order to determine the thermal lens parameters such as: θ, dn/dT, D, t_c and Peclet Number (P_E). Our results have shown that the time constant t_c , θ and peclet number P_E are very sensitive to the input pump laser power, with the increasing of the input laser powers, the t_c and Peclet number P_E have decreased, while the θ has increased as the result of laser power increase.

(Received October 16, 2023; accepted June 3, 2024)

Keywords: Thermal lens effect, Oxotrichlorobis(triphenylphosphine) rhenium(V), Thermo-optic coefficient

1. Introduction

Photo-thermal effect can be used in various chemical and physical analysis techniques[1]. This effect will be raised as results of local heating of the molecules, which led to create a refractive index gradient in the sample as the index of refraction depends on the temperature (T). The refractive index gradient changes the phase of the Gaussian laser beam profile passing through the active region. So, the active region inside the sample with a refractive index gradient can act as a converging (or diverging) lens depending on the sign of thermo-optical coefficient (dn/dT) [2]. The thermal lens (TL) technique is based on the photo-thermal effects in the presence of CW laser beam interaction with nonlinear materials. The TL technique is considered very sensitivity and simple method for studying molecular absorption spectroscopy[3, 4]. It can be applied to study the thermal physical properties of a variety of substances including solids, liquids, and gases [5]. The TL effect investigations were reported using different classes of high nonlinear optical (NLO) responses molecules, including nanoparticles [6, 7], biomedical molecules [8, 9], Fluorescein–Rhodamine B dye mixtures [10], sodium carbide nanoparticle [11], liquid ethanol [12], series of primary alcohols [13, 14], polymers [15], Functionalized multi-walled carbon nanotubes [16], and carbon fiber [17]. Also, the role of medium polarity on the NLO properties of Protoporphyrin IX [18], Eosin-B [19] and Erythrosine B dye [20] were studied.

As, the organometallic complexes with the heavy metal atoms show very high NLO responses due to the electron charge transfer between the metal coordination and the ligands. Therefore, many research groups have concentrated on studying the NLO properties of this class of materials, such as: some organometallic complex molecules [11, 21], Tris(2,2′-bipyridyl)iron(II) tetrafluoroborate [22], and dichlorobis(sarcosinato)zinc(II) complex [23].

In this study, we employed the dual-beam mode-matched CW laser z-scan configuration to investigate the TL properties of the Oxotrichlorobis(triphenylphosphine)rhenium(V) (OCPPRe). We verified that the TL effect related to the input pump laser power. Then, we extracted the thermal lens parameters of the OCPPRe including v_x, D, dn/dT, θ, t_c and Peclet number (PE) using theoretical thermal lens model.

2. Experimental techniques

The OCPPRe complex was purchased from Merck and used without any processes, Fig. 1 shows the molecular structure of OCPPRe complex, the UV-Vis absorption spectrum of the OCPPRe complex solution was taken using UV-1601PC Shimadzu spectrophotometer and it is depicted in Fig. 2. The OCPPRe complex exhibits two absorption nearby λ_1=278 nm and λ_2=416 nm due to $d \rightarrow d^*$ transitions and π-π^* transitions in the complex, respectively. The OCPPRe complex was dissolved in the benzene solvent with concentration of $2\times10^{-3}M$. The OCPPRe complex is only dissolved in polar solvent, and it has little effect on the found parameters. The used Quartz cell was 2 mm of thickness, and it was fixed in the focus (z_0=0).

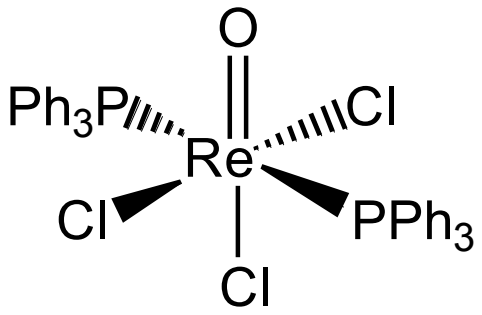

Fig. 1. Molecular structure of OCPPRe

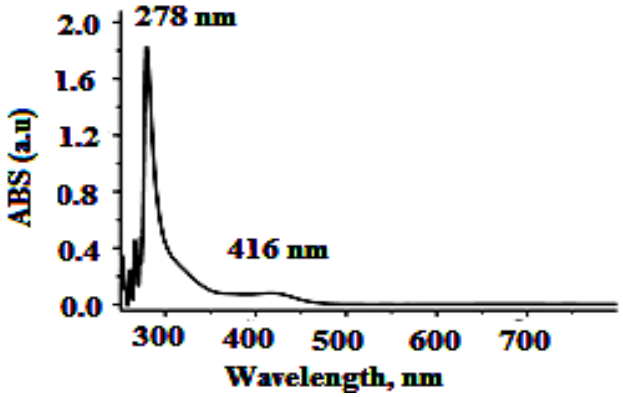

Fig. 2. UV-Vis absorption spectrum of OCPPRe

Thermal lens data were acquired using mode-matched (MM) dual-beam z-scan configuration (Schematic 1). All the experimental conditions were mentioned in our recent published works [2, 24]. A diode laser beam with λ=532 nm was used to excite the OCPPRe molecules, and a positive lens with focal point of 10 cm was used to focus the laser beam into the sample cell. The coming photons from green laser beam would be absorbed by the OCPPRe molecules; this will cause local heating to the sample molecules followed by the formation a refractive index gradient, which produces like a negative lens (thermal lens). In order to characterize the TL, low power He-Ne laser can across the active region of the TL, then the transmittance signals of He-Ne laser intensity will be changed due to formation of the TL. The TL transmittance signals were observed as a function of time (t) at different input pump powers (P_e) of 5, 10, 15, 20, 25, and 30mW.

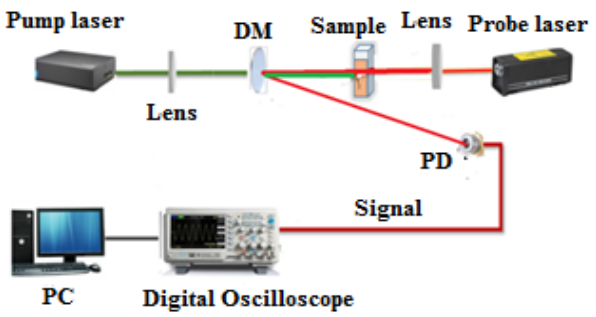

Schematic 1. Experimental setup of dual-beam z-scan (color online)

3. Results and discussion

In order to determine the TL parameters, the time resolved TL signals have to be observed, that can be performed by utilizing external pulse generator to control the on/off exposure time of the pump laser beam onto the sample. Fig. 3 shows the TL variation signals (the normalized intensity I/I_0) as a function of time at each input pump powers (P_e) of 5, 10, 15, 20, 25, and 30mW. The mean feature of experimental data gives indication that the thermal lens signals decrease with increasing the laser excitation energy [25]. Also, The recorded TL signals have shown with increasing of the input pump powers (Pe), the (t_c) would be decreased, which are in consistent with the reported works in the literature [13, 24]. In Fig. 3, all the solid lines show the best fitting of the experimental data using the numerical integration of the TL signal equation 1 [1], which includes the conductive and convective modes of heat transfer at each pump laser powers of 5, 10, 15, 20,25, and 30mW. The normalized thermal lens signals can be measured using I(t)/I(0) which I(t) and I(0) are the probe laser intensity at the detector at the time t when t = 0. In addition, in every heating cycle, I(t) is the probe beam intensity when the excitation beam is on, whereas I(0) is the probe beam intensity when the excitation beam is off. The S(t) is defined as the time resolved signal (equation 1) [1]:

$$S(t)=\frac{I(t)}{I(0)}=\left[1-\frac{i\theta}{4}\left[-\left(\frac{P_E^2}{2}\frac{(1+iV\_2m)^2}{2m(1+V)}\right)\left\{2i\tan^{-1}\left\{\frac{2mV}{\left[(1+2m)^2\right)+V^2\right]\left(\frac{t_c}{2t}\right)+1+2m+v^2}\right\}+\ln\left\{\frac{\left[1+\frac{2m}{\left(1+\frac{2t}{t_c}\right)}\right]^2+V^2}{(1+2m)^2+V^2}\right\}\right\}-P_E^2\left[\frac{2m}{(1+iV)}\ln\left(1+\frac{2t}{t_c}\right)+\left(\frac{\frac{2t}{t_c}}{1+\frac{2t}{t_c}}\right)\right]\right]^2 \quad (1)$$

The parameters in equation 1 are defined as: $m=(\omega_p/\omega_e)^2$, where ω_p and ω_e are the beam waists of the probe and the pump beams at the sample position, $v=(z/z_p)$, where z is the distance of the sample from the beam waist position of probe beam and z_p is Rayleigh range of probe beam.

The Peclet number

$$P_E = \frac{rate\ of\ convection}{rate\ of\ conduction} = \frac{\omega_e v_x}{4D} \quad (2)$$

and

$$\theta = \frac{\alpha P_e L}{k\lambda_p}\left(\frac{dn}{dT}\right) \quad (3)$$

where p_e is the pump laser power, λ_p is the wavelength of the probe beam, α is the linear absorption coefficient, L is the sample thickness, dn/dT is the thermo-optic coefficient, and k is the thermal conductivity of the solvent.The thermal diffusion time:

$$t_c = \left(\frac{\omega_e^{\ 2}}{4D}\right) \quad (4)$$

where D is the thermal diffusivity.

Our experimental data are in agreement with the theoretical thermal lens model. The OCPPRe was found to be self-defocusing media due to a negative value of the thermo-optical coefficient (dn/dT) [26], the TL effect causes the decreasing of transmitted intensity of the laser beam. Therefore, the transmitted laser intensity would decrease with the time until reaching the final steady state. Consequently, the TL signal is reduced before reaching the steady state. The amount of reduction of TL signals would depend on the rate of convection [1]. To compare the influence of convection on the TL signal of OCPPRe, we have to extract the ratio of the convective heat transfer rate to the conductive heat transfer rate (the ratio is called: Péclet Number). The values of m=43.5 and V=3.68 were calculated using the fixed experimental parameters, which will be used in the data fitting. Based on the fitting processes, the obtained parameters of dn/dT, D, v_x, t_c, PE and θ are listed in Table 1.

Table 1. Summarizes the TL parameters, tc, P_E , v_x, D, dn/dT and θ, (m=43. 5 and V=3.68 at experimental configurations).

Power (mW)	t_c (s) $\times10^{-2}$	P_E	θ	v_x(cm/s) $\times10^{-2}$	D(cm^2/s) $\times10^{-5}$	dn/dT (K^{-1})$\times10^{-3}$
5	25	0.60	0.10	1.81	5.7	1.80
10	17	0.51	0.22	2.27	8.4	2.00
15	13.9	0.43	0.35	2.34	10.3	2.12
20	11.2	0.41	0.51	2.76	12.7	2.32
25	7.5	0.35	0.63	3.47	19.2	2.29
30	6.5	0.34	0.78	3.97	21.9	2.36

The t_c and P_E have decreased with increasing the input laser power, while the θ has increased with increasing the input laser power. The values of Pectlet number (P_E) have decreased with increasing the input laser power, when P_E >1 this means the convection mode is the dominant mode of heat transfer compared to conduction in our OCPPRe, while at higher laser power starts form 15mW, at P_E<1, it means that the conduction mode is the dominant factor of heat transfer compared to convection in our sample.

The thermal Blooming (lens) will be created as results of heat generated in the local region of absorption, the refractive index will be modified and leads to negative lens (divergent lens) in our OCPPRe, which means that the sign of dn/dT is negative. When the probe laser beam passes through the absorption region and observes by the spot at far field, obviously the spot will increase in the size, and set at steady state, which was called the thermal blooming [27]. Fig. 4 shows the temporal evolution of thermal lens at pump powers of 15, 30, 50 and 90 mW using a beam profiler. The thermal lens effect develops through a period of time controlled by the exciting laser beam and characteristic of the thermal time constant of the medium [22, 28]. The temporal evolution of the thermal lens can be characterized as follow: at the time of t= 0 sec, no beam pump, the thermal lens will not be created, only we can see the profile of the probe beam. Then, at t= 1, 2 and 3 sec, the thermal lens starts to be created and having symmetrical circular feature and the thermal conduction processes predominate as the pump powers increase up to 90 mW. At the t=4 and 5 sec, the thermal lens, will be reaching the final steady state due to the studied sample reach the thermodynamic equilibrium case with the conduction and convection currents. The evolution time of the TL in Fig. 4 are in consisted with the experimental curves in Fig. 3.

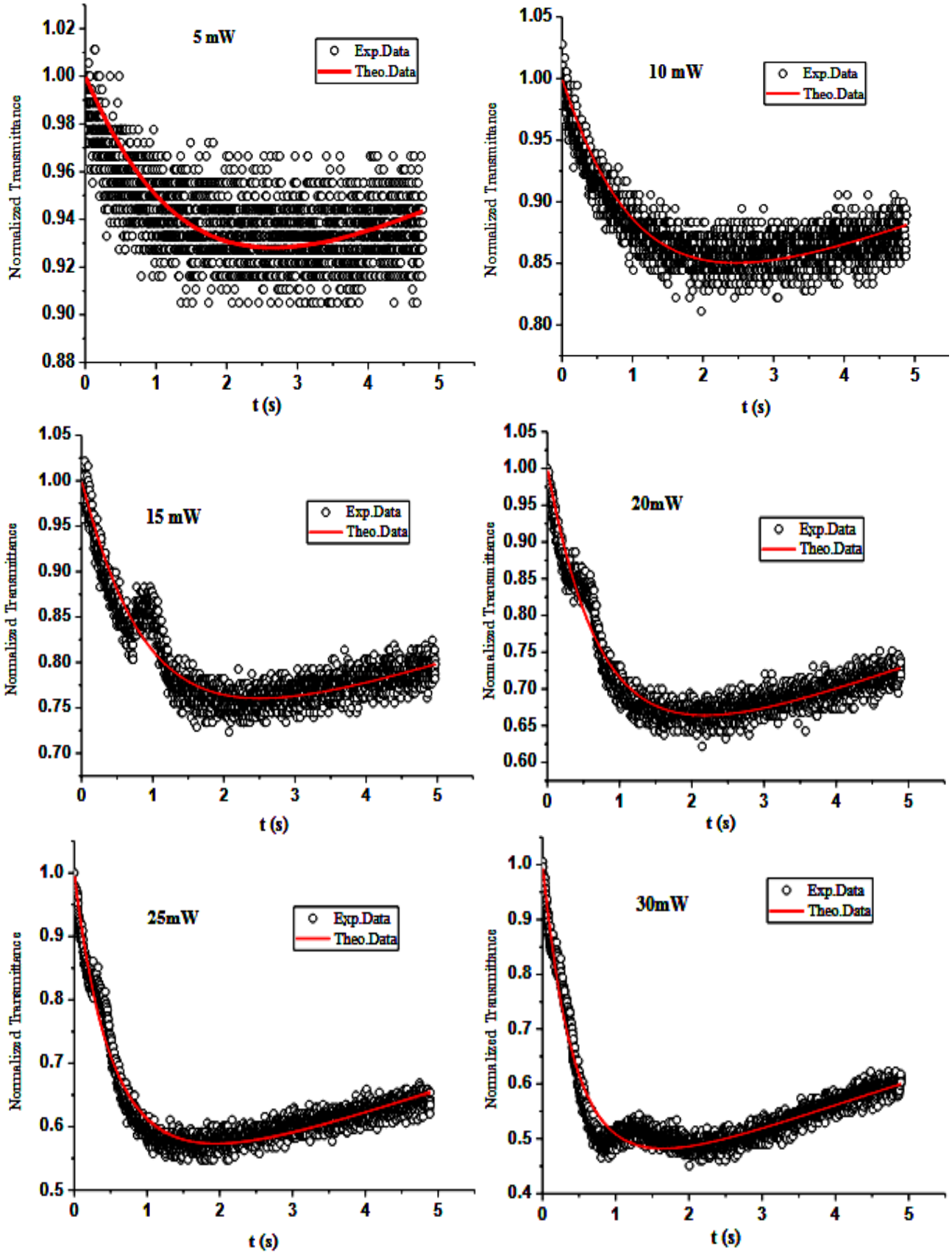

Fig. 3. The time dependence of normalized TL signals of the OCPPRe in the chloroform with concentration of 10^{-3}M at different input pump powers (back symbols). The solid lines are the best fits of the experimental data using equation (1) (color online)

Power / Time	15 mW	30 mW	50 mW	90 mW
0 sec	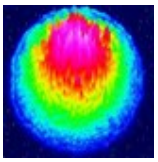	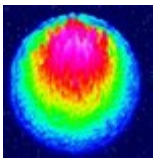	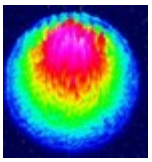	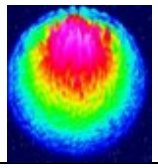
1 sec	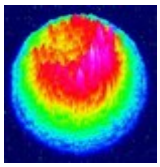	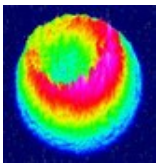	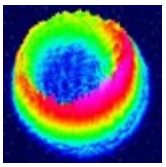	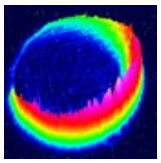
2 sec	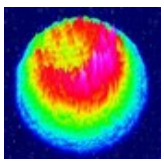	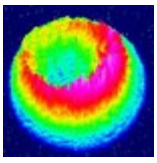	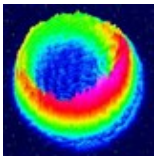	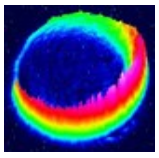
3 sec	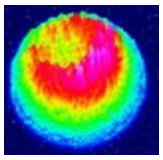	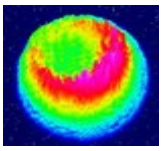	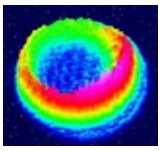	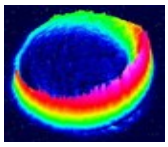
4 sec	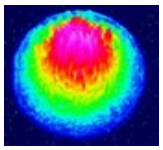	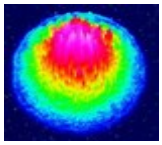	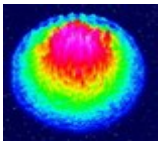	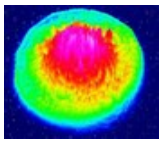
5 sec	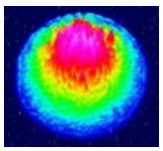	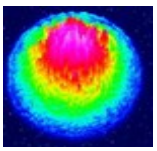	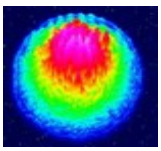	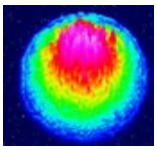

Fig. 4. TL evolution of OCPPRe (color online)

Regarding, the uncertainties in Table 1, the t_c, PE, θ, v_x, D, and dn/dT arise from the measuring of the focal spot size (±5%), linear refractive index (±0.3%), linear absorption coefficient (±5%) and Rayleigh length (±4%). The maximum error bar to be estimated less than 5% for each parameter.

4. Conclusion

We have employed the CW mode-matched dual beams (pump-probe) TL configuration for studying the TL properties of OCPPRe solution. The observed TL signals are increased linearly with the laser pump power, as results of strong absorption inside the sample, which has led to rise of TL effect. The thermal lens model was applied to extract the TL parameters (dn/dT, D, v_x, tc, PE and θ). Our results show the contribution of convective and conduction heat transfer in the thermal lens effect was quantified in terms of the Péclet Number (P_E). The temporal evolution of TL was observed over period of time at input pump power of 15, 30, 50 and 90 mW.

Acknowledgements

We would like to the AEC of Syria for the financials support. Also, our thank goes to Prof. I. Othman; the head of AECS and Prof. M. K. Sabra for their valuable help.

References

[1] S. Singhal, D. Goswami, Analyst **145**, 929 (2020).

[2] A. Ghanem, M. D. Zidan, M. S. El-Daher, A. Allahham, Optik **252**, 168499 (2022).
[3] E. Dy, C. Gu, J. Shen, W. Qu, Z. Xie, X. Wang, M. L. Baesso, N. G.C. Astrath, Journal of Applied Physics **131**(6) 063102 (2022).
[4] M. Liu, Thermochimica Acta **672**, 126 (2019).
[5] N. Nossir, L. Dalil-Essakali, A. Belafhal, Optik **166**, 323 (2018).
[6] S. Adhikari, P. Spaeth, A. Kar, M. D. Baaske, S. Khatua, M. Orrit, ACS Nano **14**, 16414 (2020).
[7] Z.-C. Zeng, H. Wang, P. Johns, G. V. Hartland, Z. D. Schultz, Journal of Physical Chemistry C 121, 11623 (2017).
[8] G. Mazza, T. Posnicek, L.-M. Wagner, J. Ettenauer, K. Zuser, M. Gusenbauer, M. Brandl, Sensors and Actuators B: Chemical **249**, 731 (2017).
[9] E. Cedeño, H. Cabrera, A. E. Delgadillo-López, O. Delgado-Vasallo, A. M. Mansanares, A. Calderón, E. Marín, Talanta **170**, 260 (2017).
[10] A. Kurian, S. D. George, V. P. N. Nampoori, C. P. G. Vallabhan, Spectrochimica Acta Part A: Molecular and Biomolecular Spectroscopy **61**, 2799 (2005).
[11] M. S. Swapna, S. Sankararaman, International Journal of Thermophysics **41**, 93 (2020).
[12] M. H. Mahdieh, M. A. Jafarabadi, E. Ahmadinejad, Proc. SPIE **9255**, 31(2015).
[13] S. Singhal, D. Goswami, ACS Omega **4**, 1889 (2019).
[14] P. Kumar, A. Khan, D. Goswami, Chemical Physics **441**, 5 (2014).
[15] X. Chen, Y. Su, D. Reay, S. Riffat, Renewable and Sustainable Energy Reviews **60**, 1367 (2016).
[16] Y. Guo, K. Ruan, X. Yang, T. Ma, J. Kong, N. Wu, J. Zhang, J. Gu, Z. Guo, Journal of Materials Chemistry C **7**, 7035 (2019).
[17] W. Si, J. Sun, X. He, Y. Huang, J. Zhuang, J. Zhang, V. Murugadoss, J. Fan, D. Wu, Z. Guo, Journal of Materials Chemistry C **8**, 3463 (2020).
[18] M. Hoseini, A. Sazgarnia, S. Sharifi, Journal of Fluorescence **29**, 531 (2019).
[19] N. Karimi, S. Sharifi, S. S. Parhizgar, S. M. Elahi, Optical and Quantum Electronics **50**, 209 (2018).
[20] M. Pourtabrizi, N. Shahtahmassebi, A. Kompany, S. Sharifi, Optical and Quantum Electronics **50**, 13 (2017).
[21] G. Argüello-Sarmiento, M. Ortiz-Gutiérrez, M. Trejo-Durán, J. A. Andrade-Lucio, J. E. Castellanos-Águila, E. Alvarado-Méndez, Journal of Molecular Liquids **383**, 122058 (2023).
[22] M. D. Zidan, M. M. Al-Ktaifani, M. S. El-Daher, A. Allahham, A. Ghanem, Optoelectronics Letters **17**, 183 (2021).
[23] S. Chitrambalam, S. Abraham, V. K. Rastogi, I. Hubert Joe, Chemical Physics Letters **754**, 137648 (2020).
[24] M. D. Zidan, A. Arfan, M. S. EL-Daher, A. Allahham, A. Ghanem, D. Naima, Optical Materials **117**, 111133 (2021).
[25] M. R. Mohebbifar, Measurement **156**, 107611 (2020).
[26] M. D. Zidan, A. W. Allaf, A. Allaham, A. Al-Zier, Optik **283**, 170939 (2023).
[27] S. A. Joseph, M. A. Hari, S. Mathew, G. Sharma, Soumya, V. Hadiya, P. Radhakrishnan, V. P. N. Nampoori, Optics Communications **283**, 313 (2010).
[28] H. A. Badran, Results in Physics **4**, 69 (2014).

*Corresponding author: PScientific8@aec.org.sy